JOURNAL OF Materials CHEMISTRY

The layered perovskite $K_2SrTa_2O_7$: hydration and K^+/H^+ ion exchange†

Marie-Pierre Crosnier-Lopez, Françoise Le Berre and Jean-Louis Fourquet*

Laboratoire des Fluorures, (UMR 6010, CNRS), Faculté des Sciences du Mans, Université du Maine, Avenue O. Messiaen, 72085 Le Mans Cedex 9, France

Received 17th July 2000, Accepted 19th December 2000
First published as an Advance Article on the web 9th February 2001

We present a full characterization of the anhydrous layered material $K_2SrTa_2O_7$ related to Ruddesden–Popper type phases. The unit cell, determined from powder X-ray diffraction, is tetragonal with $a=3.9858(1)$ Å and $c=21.785(1)$ Å (space group $I4/mmm$, $Z=2$). The layered structure allows spontaneous water intercalation when the product is kept in air at ambient temperature. During hydration, a reversible structural transformation from an I to a P Bravais lattice is observed. By using K^+/H^+ ion exchange, in dilute HNO_3 or in acetic acid, we obtained the protonated phase $H_2SrTa_2O_7{\cdot}xH_2O$ which is compared to the one synthesized from $Li_2SrTa_2O_7$ previously reported by us. For both compounds, the hydration–dehydration behavior, studied by DTA/TGA and X-ray thermodiffractometry is discussed. In addition, we carried out an electron microscopy study of anhydrous $K_2SrTa_2O_7$ by selected area electron diffraction (SAED).

Introduction

We have recently reported the synthesis and crystal structure of new oxides of general formula,[1,2] $Li_2A_{0.5n}B_nO_{3n+1}$ (A = Ca, Sr; B = Nb, Ta), which belong to a family of oxides related to the layered perovskites of the Ruddlesden–Popper (RP) type. Since RP phases are well known to show ion exchange behavior,[3] we have also prepared the protonated phases $H_2A_{0.5n}B_nO_{3n+1}$ by ion exchange in dilute HNO_3 at 60 °C;[4] this exchange obeys a topotactic mechanism since the layered structure is preserved. All the protonated phases present both a considerable expansion of the c-parameter and a change in the Bravais lattice (from I to P) of the unit cell with a broadening of some diffraction lines. Despite our efforts, we have not succeeded in solving the room temperature structures. Upon heating, a rapid shrinking of the c-parameter accompanied by a reverse from a primitive to a centered cell is observed. During the dehydration process, we expected the formation of novel metastable 3-D perovskites $A_{0.5}BO_3$ with exotic ordering vacancies. A structural view of these hypothetical $A_{0.5}BO_3$ phases is given as ESI.† Unfortunately, the dehydration leads to the formation of disordered phases as revealed by the HREM images observed for $Sr_{0.5}TaO_3$.[4] These metastable disordered phases $A_{0.5}BO_3$ finally transform systematically to the thermodynamically stable AB_2O_6 compounds, providing a low temperature route for their synthesis.

During this work one paper in particular held our attention, published by Ollivier and Mallouk,[5] concerning the ion exchange $K^+ \leftrightarrow H^+$ on $K_2SrTa_{2-x}Nb_xO_7$ ($x=0.0$, 0.2, 0.4) during the preparation of the metastable phase $SrTa_{2-x}Nb_xO_6$. They showed that the X-ray diffraction pattern of $H_2SrTa_{1.6}Nb_{0.4}O_7$ ($x=0.4$) can be indexed in a tetragonal cell with an a-parameter close to a_p and a c-parameter halved upon proton exchange ($\approx$9.87(18) Å). They associate this situation to a lateral shift of alternate layers, leading to (Ta,Nb)O_6 octahedra facing each other. Taking into account the perovskite layer thickness ($\approx$7.78 Å), this would imply O–O distances close to 2.09 Å, which seems very unlikely. However, it is interesting to note that as in our compounds $Li_2A_{0.5n}B_nO_{3n+1}$, the exchange obeys a topotactic mechanism.

The aim of this work is to check if the two $H_2SrTa_2O_7$ compounds obtained by ion exchange from the Li and K phases have the same structures and if their dehydration leads to the same metastable phases before their final transformation.

At least we began this work with the structural characterization of the starting compound $K_2SrTa_2O_7$, which was not carried out by Ollivier and Mallouk.[5]

Experimental

Pure $K_2SrTa_2O_7$ and $K_2SrTa_{1.6}Nb_{0.4}O_7$ samples were synthesized by a conventional solid state method: stoichiometric quantities of strontium carbonate, tantalum oxide, niobium oxide and an excess (40% for $K_2SrTa_2O_7$ and 60% for $K_2SrTa_{1.6}Nb_{0.4}O_7$) of dried potassium carbonate were ground and then pressed into a pellet. This was then placed on a platinum plate fired in air (at a heating rate of 10 °C min^{-1}) at 850 °C for 6 hours and then at 1050 °C for 6 hours. For $K_2SrTa_{1.6}Nb_{0.4}O_7$, a first heating at 850 °C for 6 hours followed by grinding was needed. The final heating was followed by natural cooling to 200 °C in order to avoid hydration of the phases.

Thermal analysis, thermogravimetric (TG) analysis coupled with differential thermal (DT) analysis of the hydrated layered oxide and of the proton derivatives was made using a TA Instruments SDT 2960 system operating with a heating rate of 5 to 10 °C min^{-1} under a flowing argon atmosphere. X-Ray thermodiffractometry using a Siemens D5000 diffractometer (Cu-Kα radiation) was carried out under a helium flow to study the dehydration process of $K_2SrTa_2O_7{\cdot}xH_2O$ and of the proton exchanged compound with the following conditions: 2θ range 6 to 80°, heating rate 5 °C min^{-1}, delay time 5 min, step scan 0.03°, step time 22 s.

The powder X-ray diffraction (PXRD) patterns were recorded at room temperature using a Siemens D-500 diffractometer (Cu-Kα radiation) in the 2θ range 5 to 130° (step scan 0.02°, step time 40 s). In order to avoid the hydration

†Electronic supplementary information (ESI) available: a structural view of the hypothetical $A_{0.5}BO_3$ phases, a TGA plot and thermo X-ray diffractogram for $K_2SrTa_2O_7{\cdot}xH_2O$ and a thermo X-ray diffractogram for $H_2SrTa_2O_7{\cdot}xH_2O$. See http://www.rsc.org/suppdata/jm/b0/b005755j/

 DOI: 10.1039/b005755j

process, a hot sample holder (200 °C) was used to record the X-ray powder pattern of the anhydrous form.

Transmission electron microscopy (TEM) studies (electron diffraction (ED)) were carried out using a JEOL 2010 electron microscope operating at 200 kV and equipped with a side entry $\pm 30°$ double tilt specimen holder. The anhydrous $K_2SrTa_2O_7$ sample was ultrasonically dispersed in hexane and a drop of the suspension was placed on a Cu grid with a holey carbon film.

$K_2SrTa_2O_7$: Results and discussion

Structural determination: powder X-ray diffraction and TEM study

$K_2SrTa_2O_7$ allows spontaneous water intercalation when exposed to air under ambient conditions as already encountered for $K_2Nd_2Ti_3O_{10}$.[6] The PXRD pattern was recorded at 200 °C (Fig. 1). All the observed lines could be indexed on a tetragonal cell with $a = 3.9858(1)$ Å, $c = 21.785(1)$ Å, the systematic absences showing body centering leading to the extinction symbol I^-. The Rietveld method with the Fullprof[7] program was used to refine the structure in the space group *I*4/*mmm* (no. 139) with a starting model for the perovskite slabs similar to that observed in the lithium phase. Then, one site was found for the K atoms allowing completion of the structure. For the final refinement, with 18 parameters and 266 reflections, the conventional reliability factors R_p, R_{wp}, R_{exp}, and R_B converge to 0.119, 0.121, 0.024 and 0.053 respectively. Final parameters and selected interatomic distances are collected in Tables 1 and 2.

In order to confirm the results obtained from the powder X-ray diffraction experiments, we carried out an electron microscopy study of anhydrous $K_2SrTa_2O_7$ by selected area electron diffraction (SAED). Two typical SAED patterns of the (001) and (010) orientations for $K_2SrTa_2O_7$ are shown in Fig. 2.

Most of the crystallites are very thin platelets with the *c*-axis parallel to the electron beam, giving a (001) plane with a first order Laue zone which was widened due to the high value of the *c*-parameter and the thickness of the sample (Fig. 2a). Reciprocal space always leads to a tetragonal unit cell with $a \approx 3.9$ Å and $c \approx 21.8$ Å, revealing no superstructure. The (001) plane clearly shows additional spots (Fig. 2a) which appear at the extinct positions (*h*00, with *h* odd): they can be attributed without any doubt to double diffraction from the first order Laue zone. As a matter of fact, they do not appear in the (010) plane (Fig. 2b). These results are in good agreement with those obtained from the powder X-ray diffraction study.

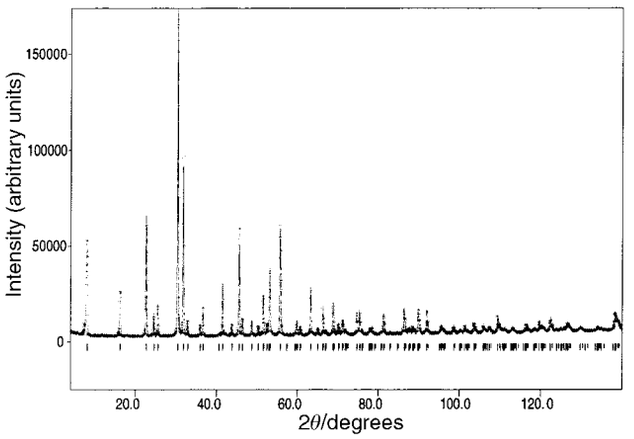

Fig. 1 Observed (···) and calculated (—) powder X-ray diffraction patterns of $K_2SrTa_2O_7$ ($n = 2$) at 200 °C [space group *I*4/*mmm* (no. 139)]. The difference pattern is shown below at the same scale (vertical bars are related to the calculated Bragg reflections).

Table 1 Atomic parameters from the Rietveld refinement of $K_2SrTa_2O_7$ at 200 °C[a]

Atoms	*x*	*y*	*z*	*B*/Å^2	Site
Ta	0	0	0.40372(4)	0.23(1)	4e
Sr	0	0	0	0.92(5)	2a
K	0	0	0.1934(1)	0.40(8)	4e
O1	0.5	0	0.0862(3)	1.0(1)	8g
O2	0.5	0.5	0.1798(3)	1.0(1)	4e
O3	0	0	0.5	1.0(1)	2b

[a]Space group *I*4/*mmm* (no. 139), $a = 3.9858(1)$ Å, $c = 21.785(1)$ Å, $Z = 2$, $R_p = 0.119$, $R_{wp} = 0.121$, $R_{exp} = 0.024$; $R_b = 0.053$.

Table 2 Main distances (Å) and calculated bond valences

Ta^{5+} octahedra	Sr^{2+} polyhedra	K^+ polyhedra
$1 \times 1.810(7)$	$8 \times 2.739(5)$	$1 \times 2.763(7)$
$4 \times 2.006(7)$	$4 \times 2.818(1)$	$4 \times 2.834(1)$
$1 \times 2.107(10)$		$4 \times 3.069(5)$

Atoms	O1	O2	O3	Σ	Σexp[a]
Ta	0.62	1.31	0.79×4	5.09	5
K		$0.18 + 0.15 \times 4$	0.08×4	1.10	1
Sr	0.15×4		0.19×8	2.12	2
Σ	1.84	2.09	1.78		
Σexp	2	2	2		

[a]$Si = \Sigma j \exp[(R_{ij} - d_{ij})/0.37]$ and R_{ij} for O^{2-} is 1.920 for Ta^{5+}, 2.118 for Sr^{2+} and 2.130 for K^+.[14]

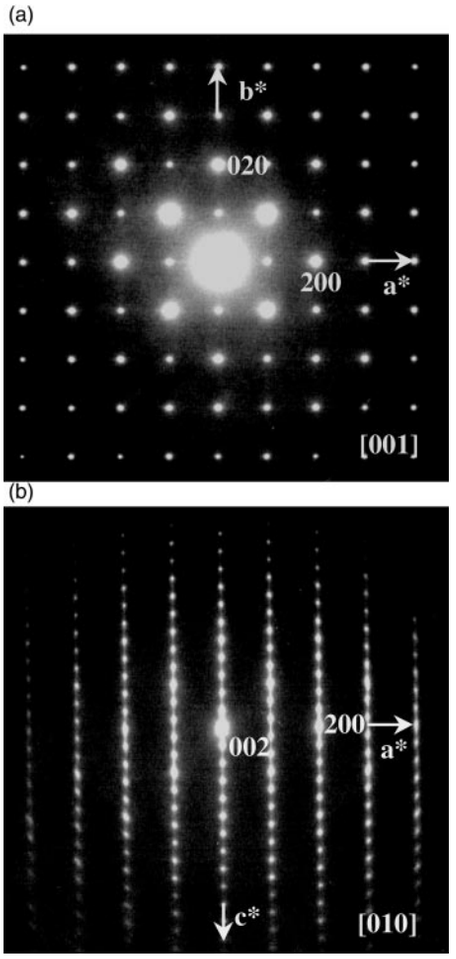

Fig. 2 Two sections of the reciprocal space for anhydrous $K_2SrTa_2O_7$: (a) (001) and (b) (010) zone axis.

Structural description

The structure of anhydrous $K_2SrTa_2O_7$ (Fig. 3) can be described as formed from two TaO_6 octahedra thick slabs of a perovskite lattice cut along the *c* direction; these alternate layers are shifted by $(a+b)/2$ (body centered), with the large Sr cations fully occupying the 12-coordinated sites. The potassium ions, classically found to occupy the interlayer spacing, are located in a mono-capped square antiprism (C.N. = 9) as already observed in K_2NiF_4.[8] It is interesting to note that in the two potassium and lithium derivatives, the same relative arrangement of two adjacent perovskite sheets is observed, despite the difference between the two ionic radii of the A^+ ions. This stacking feature is in complete agreement with that found in the titanate compounds $ALaTiO_4$ (A = Li, Na, Ag),[9–12] but is in contrast to that in $ALaTa_2O_7$,[13] in which the relative arrangement is dependent on the A^+ ion size. In the potassium compound, the adjacent perovskite layers are stacked with a displacement of ½ along only one direction within the layer plane, *i.e.* the [100] direction in the space group *C*222, while in the lithium ion exchanged compound the displacement observed is by ½ along the [110] direction.

The tantalum atoms are displaced from the center of the octahedron so that three Ta–O bonds can be classified: a short bond toward the interlayer spacing (1.810 Å), an opposite long bond (2.107 Å) and four equal equatorial bonds within the perovskite layers (2.006 Å). The mono-capped antiprism [KO_9] involves three different K–O bonds (1×2.763 Å, 4×2.834 Å and 4×3.069 Å). The shortest one (2.763 Å) is observed with the terminal oxygen atom O2 of the nearest TaO_6 octahedron belonging to the adjacent slab. The Sr–O distances, ranging from 2.739 to 2.818 Å, and the observed K–O bonds are in good agreement with the values found in the literature.[2,7,13] In order to check our results, we decided to use the valence bond method:[14] for each cationic and anionic site, the atomic charge was determined and all the results gathered in Table 2 are in good agreement with the expected values.

Concerning the $K_2SrTa_{1.6}Nb_{0.4}O_7$ compound, the powder X-ray diffraction diagram, collected at 200 °C, is similar to that of $K_2SrTa_2O_7$. All the observed lines can be indexed on a tetragonal cell with $a = 3.9858(5)$ Å and $c = 21.782(3)$ Å refined by the Eracel program.[15] As expected, these cell parameters are very close to those of $K_2SrTa_2O_7$ ($r_{Ta^V} = r_{Nb^V} = 0.64$ Å).[16]

Water intercalation

We quickly observed that $K_2SrTa_2O_7$ allows spontaneous water absorption when exposed to air under ambient conditions. The mass variation during the rehydration of anhydrous $K_2SrTa_2O_7$ has been studied by maintaining the product under an air flow at room temperature (humidity rate: 70%, see the ESI†). After three days no saturation is visible and the absorbed water content leads to the formula $K_2SrTa_2O_7\cdot2.90H_2O$. Simultaneously to TGA measurements, X-ray diffractometry was used to follow the water absorption and to determine if the weight increase was due to water intercalation, water adsorption or both. Fig. 4 shows the evolution of the powder X-ray diffraction pattern for anhydrous $K_2SrTa_2O_7$ *versus* exposure time to air at room temperature. New reflection lines associated with the hydrated form appear rapidly while the diffraction peaks of the anhydrous $K_2SrTa_2O_7$ decrease. We deduced from these observations that $K_2SrTa_2O_7$, thanks to its layered structure, spontaneously intercalates water. However, we can't completely exclude a simultaneous adsorption. The first step, where both anhydrous and hydrated phases coexist, corresponds to the beginning of the TGA curve when the weight increase is very fast. After seven hours under air, the anhydrous form completely disappeared and the corresponding formula of the hydrated form is $K_2SrTa_2O_7\cdot1.56H_2O$. The hydration process then becomes slower. For longer exposure to air and in agreement to the TGA experiment, no saturation occurs even after one week as shown by the continuous evolution of the diffraction pattern. In addition, we observe a loss of crystallinity with, in particular, a widening of the (00*l*) reflection lines as the water content increases. It probably corresponds to an amorphization due to a disorder increase between the slabs as suggested by Richard *et al.*[6] These disordered phases apparently still contained well organized perovskite layers as evidenced by the presence of thin (*hk*0) reflections. In order to determine the structure of the hydrated phase, a PXRD pattern was collected at room temperature on a sample exposed to air for nine hours. For such exposure times, the X-ray diagram probably corresponds to that of a product of a well defined hydrated phase presenting a relatively good crystallinity. All the lines can be indexed on the basis of a tetragonal cell with the *a*-parameter close to that of the anhydrous phase and a careful examination of the indexing showed that the diffractogram could be indexed on a primitive cell ($a = 3.961(1)$ Å and $c = 12.745(3)$ Å). Despite our efforts, we did not succeed in refining the structure, probably due to the hydration process which continues during the X-ray data collection. However, this kind of structural transformation (body centered to primitive lattice), associated with the hydration process, has already been observed in layered perovskites[3,6] and has been

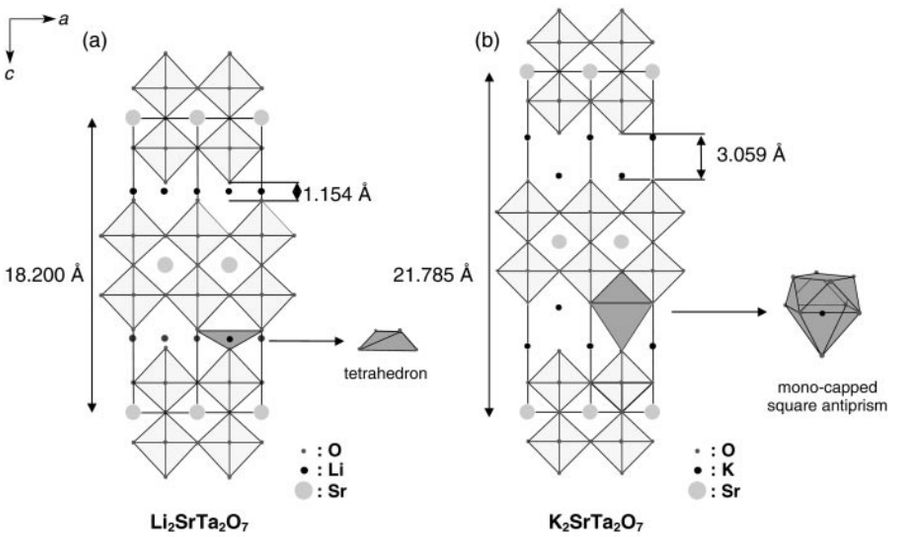

Fig. 3 Projection of the crystal structure of $Li_2SrTa_2O_7$ (a) and $K_2SrTa_2O_7$ (b) showing the perovskite lattice (2-TaO_6 octahedra) and the coordination polyhedron of the alkaline ions.

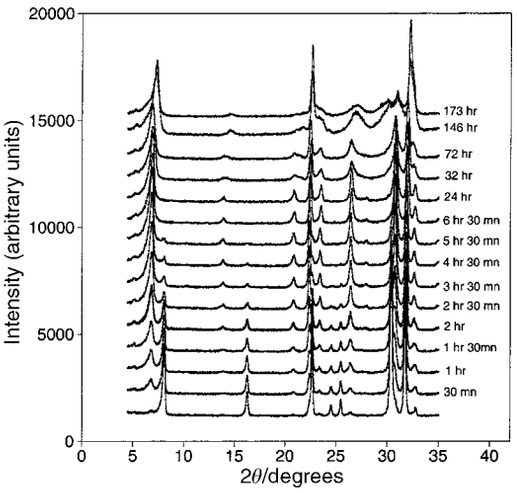

Fig. 4 $K_2SrTa_2O_7$ powder X-ray diffraction pattern evolution *versus* exposure time to air (humidity rate: 70%) showing the rehydration process.

attributed to a shift of alternate layers. The adjacent layers are stacked immediately above each other in the same arrangement leading to a halving of the *c*-axis length upon hydration. Thermo X-ray diffractometry measurements (see the ESI)† allow us to observe that the centered lattice of the anhydrous phase can be restored by heating the hydrated form. For $T<270\,^{\circ}C$, only peaks relative to the hydrated form are visible while for $T>430\,^{\circ}C$, we only observe the anhydrous phase $K_2SrTa_2O_7$. Between these two temperatures, the two forms coexist as already mentioned. It must be pointed out that the peaks related to the anhydrous form between 270 and 570 °C are slightly shifted toward low 2θ in comparison to those observed at room temperature. This fact can be explained by the thermal expansion of the cell parameters. Surprisingly, the structural transformation ($P\rightarrow I$) is not correlated with a peak on the TGA/DTA curve probably due to a continuous phase transition (Fig. 5). We observe two distinct important losses of water with only one endothermic peak associated with the first loss. This peak, ($T<200\,^{\circ}C$), may be due to the dehydration of a disordered hydrate leading to a well crystallized hydrated compound. Then for $200\,^{\circ}C<T<400\,^{\circ}C$, the two forms — anhydrous and hydrated — coexist. For higher temperatures, only the anhydrous form exists.

For the $K_2SrTa_{1.6}Nb_{0.4}O_7$ compound, the capacity to absorb/desorb water was also observed with apparently the same structural transformation, $I\leftrightarrow P$. In comparison to $K_2SrTa_2O_7$ the hydration proceeds more slowly, about 20 hours elapse before the beginning of the hydration process

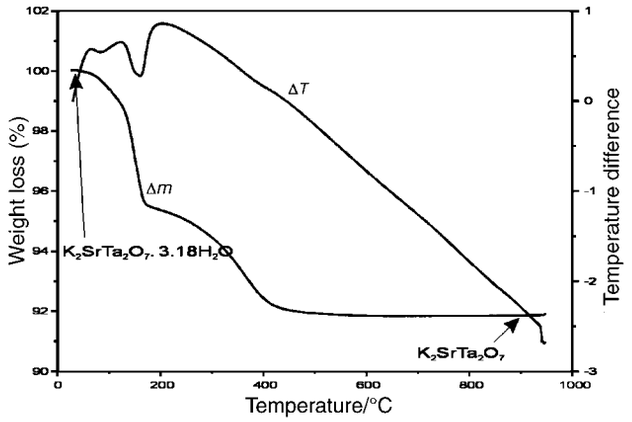

Fig. 5 DTA and TGA curves showing the dehydration process for $K_2SrTa_2O_7\cdot xH_2O$.

is detected. As for the pure tantalum phase, $K_2SrTa_{1.6}Nb_{0.4}O_7\cdot xH_2O$ diffraction spectra show a strong amorphization preventing any accurate structural refinement.

K^+/H^+ ion exchange: $H_2SrTa_2O_7$

The K^+/H^+ exchange was realized respectively on anhydrous $K_2SrTa_2O_7$ and $K_2SrTa_{1.6}Nb_{0.4}O_7$. For each test, the solid was washed with distilled water, and finally with acetone before drying in air at room temperature; the K content analysis of the filtrate was performed using flame photometry.

HNO_3 solutions. As reported earlier,[4] 1 g portions of the parent oxides were added to 100 ml of 2 M HNO_3 maintained at room temperature or around 60 °C for one day with constant stirring. The exchange is complete at this point but the crystallinity of the obtained material is low compared to that obtained from Li^+/H^+ exchange on $Li_2SrTa_2O_7$ [4] (Fig. 6a). We then tried lower HNO_3 molarities but, despite complete exchange occurring, the crystallinity was not improved. Therefore, we decided to exchange $K_2SrTa_2O_7$ with a less strong acid such as CH_3COOH.

Acetic acid. The reaction was realized by refluxing (140 °C) 0.5 g of anhydrous $K_2SrTa_2O_7$ in 300 ml of CH_3COOH for one day. As for HNO_3 solutions, the exchange was complete but the crystallinity remained the same.

Since the exchange is complete regardless of the mother phase, only the results concerning the K^+/H^+ exchange performed on $K_2SrTa_2O_7$ are presented.

The DTA/TGA curves of different $H_2SrTa_2O_7\cdot xH_2O$ samples always exhibit multi-step weight loss behavior which could be related to the formation of discrete structural intermediates during the dehydration reaction. Surprisingly, this multi-step behavior is not associated with any thermal phenomena, probably due to a continuous dehydration process (Fig. 7a). However, the total weight loss, beginning at 50 °C and depending on the protonated compound studied, is always

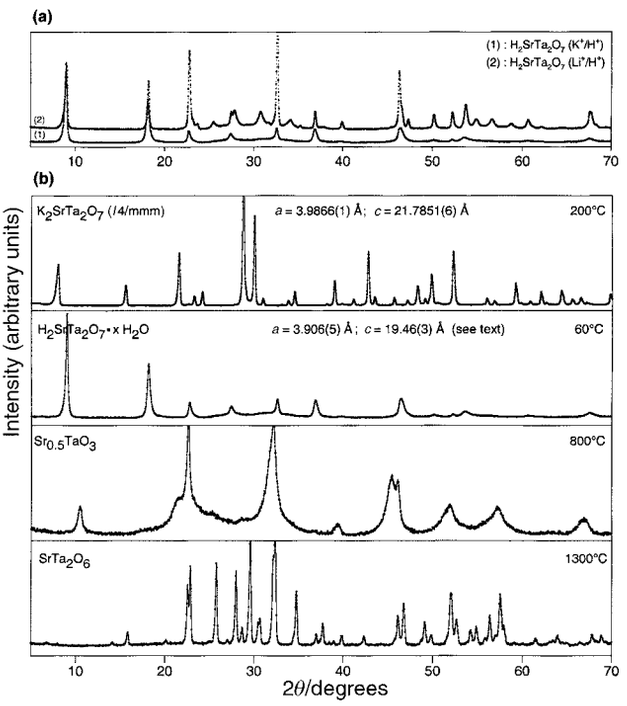

Fig. 6 (a) Comparison between the powder X-ray diffraction patterns of $H_2SrTa_2O_7$ prepared from $K_2SrTa_2O_7$ and from $Li_2SrTa_2O_7$. (b) Powder X-ray diffraction patterns of $H_2SrTa_2O_7\cdot xH_2O$ at different temperatures during transformation. In comparison, the PXRD pattern of the mother phase, $K_2SrTa_2O_7$, is also given.

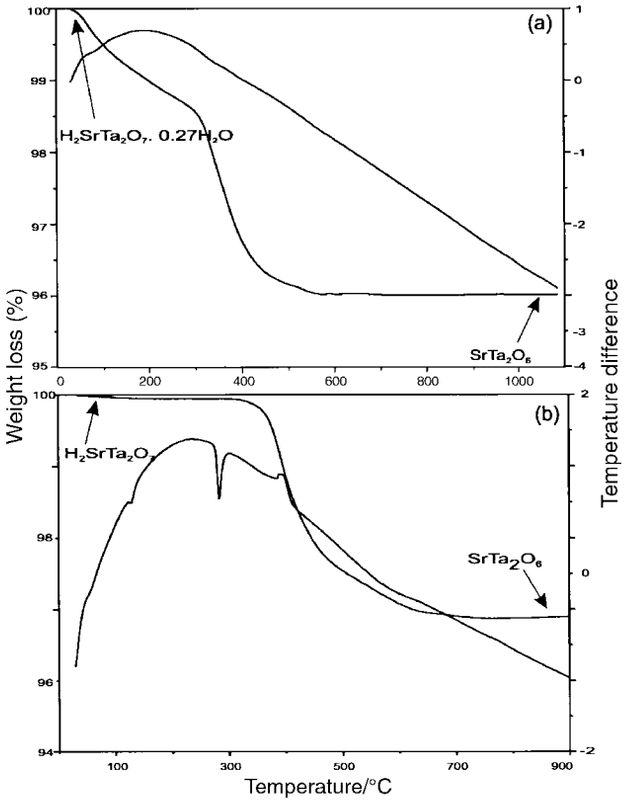

Fig. 7 DTA and TGA curves showing the dehydration process for $H_2SrTa_2O_7$ prepared from $K_2SrTa_2O_7$ (a) and from $Li_2SrTa_2O_7$ (b).

larger than the calculated one for the anhydrous form $H_2SrTa_2O_7$ (3.2%), implying that the space between the layers is occupied by variable amounts of water. As an example, the total weight loss observed on Fig. 7a (completed at about 600 °C) corresponds to 1.27 H_2O, leading to the starting formula $H_2SrTa_2O_7 \cdot 0.27H_2O$. This result is not surprising and can be explained by the easy water intercalation in the mother phase, $K_2SrTa_2O_7$; the ionic K^+/H^+ exchange, achieved in aqueous solution, is then performed on the hydrated form $K_2SrTa_2O_7 \cdot xH_2O$ in which the perovskite layers are more separated than in the anhydrous variety.

In the case of $H_2SrTa_2O_7$ prepared from the Li mother phase[4] (Fig. 7b), only one weight loss was observed (3.2%) corresponding to the loss of one proton as H_2O. It leads to the $SrTa_2O_6$ compound as confirmed by X-ray measurements. We deduced that $H_2SrTa_2O_7$ obtained by Li^+/H^+ exchange is anhydrous contrary to the one obtained from $K_2SrTa_2O_7 \cdot xH_2O$.

As one can see from Fig. 6a, all the lines of the protonated phase obtained from $K_2SrTa_2O_7$ correspond to the strongest ones of the exchanged Li phase. Since the two mother phases (K and Li) have the same relative arrangement of the perovskite blocks (body centered), and the proton exchange clearly obeys a topotactic mechanism, the same protonated phase would be expected. From a careful examination of the powder X-ray diffraction pattern, we noticed the presence of strong (00*l*) lines indicating that the layered structure is preserved while two peaks characteristic of the perovskite blocks ($d = 3.924$ and 1.960 Å) are observed. A pattern matching refinement is then carried out using a tetragonal cell [$a \approx 3.906(5)$ Å and $c \approx 19.46(3)$ Å], (Rietveld method using the Fullprof program[7]) and allows all the lines to be indexed. However, we did not succeed in refining the structure due to the poor crystallinity of the sample. Taking into account these observations, we are not able to conclude if these two protonated phases have exactly the same structure. It must be pointed out that according to the study of Ollivier and Mallouk,[5] a pattern matching refinement was attempted with a tetragonal a_p cell and a halved *c*-parameter (≈ 9.73 Å): the result is not satisfactory since some reflections cannot be indexed.

In order to see the changes occurring on heating, we carried out thermo-X-ray diffractometry on $H_2SrTa_2O_7 \cdot xH_2O$, (see the ESI).† Surprisingly, despite the multi-step weight loss but similarly to the DTA/TGA curves, the X-ray diffraction patterns reveal a continuous evolution between 50 and 250 °C, with no distinct structural intermediate as a hypothetical anhydrous $H_2SrTa_2O_7$ form: the loss of xH_2O and the loss of protons as H_2O occurs simultaneously leading to the metastable phase $Sr_{0.5}TaO_3$. At 800 °C (Fig. 6b), the powder X-ray diffraction pattern of this compound still presents a broad line at low 2θ values (close to 10.5°) corresponding to $d \approx 8.4$ Å. This fact indicates that the final 3-D condensation is not complete. Taking into account the broadening of the lines when the temperature increases, we deduce that the disordered perovskite formation occurs as for the dehydration process of $H_2SrTa_2O_7$ prepared from $Li_2SrTa_2O_7$. A rapid change appears at about 1000 °C yielding to the thermodynamically stable $SrTa_2O_6$ (pure Tetragonal Tungsten Bronze TTB form).[17] In the case of $H_2SrTa_2O_7$ prepared from $Li_2SrTa_2O_7$,[4] this transformation takes place at about 942 °C and yields mainly the TTB form $SrTa_2O_6$ with a small amount of an orthorhombic variety.[18]

As in the case of the other protonated phases prepared from layered $Li_2A_{0.5n}B_nO_{3n+1}$ perovskite materials,[4] the expected formation of a novel metastable three-dimensional and vacancies ordered A-site deficient perovskite $A_{0.5}BO_3$ (ESI)† does not seem to occur.

Conclusion

During this work, we have fully characterized, by powder X-ray diffraction, the anhydrous layered material $K_2SrTa_2O_7$, related to Ruddlesden–Popper phases. Its structure can be described as formed from a perovskite lattice of two thick TaO_6 octahedral slabs, cut along the *c* direction. These alternate layers are shifted by $(a+b)/2$ (body centered). This 2-D natural structure allows spontaneous water intercalation when the product is kept under air. A reversible structural transformation, centered to a primitive tetragonal cell, is observed. However, as soon as the anhydrous form has completely disappeared, a loss of crystallinity is quickly observed preventing the structural determination of the hydrated form. The protonated phase $H_2SrTa_2O_7 \cdot xH_2O$ can be easily prepared by K^+/H^+ ion exchange from $K_2SrTa_2O_7$. This exchange clearly obeys a topotactic mechanism since the layered structure is preserved. As for the mother phase, the exchanged product $H_2SrTa_2O_7 \cdot xH_2O$ is always hydrated, contrary to $H_2SrTa_2O_7$ prepared from the acid exchange of $Li_2SrTa_2O_7$. Owing to the low crystallinity of this compound, all our attempts to solve the room temperature structure were unsuccessful as for $H_2SrTa_2O_7$ obtained by Li^+/H^+ exchange.[4] The X-ray study only allowed us to conclude that in addition to the preservation of the layered structure, the perovskite blocks are still present. After dehydration, both protonated phases transform upon heating into a disordered $Sr_{0.5}TaO_3$ metastable phase initially and to a thermodynamically stable $SrTa_2O_6$ phase at higher temperatures.

References

1 N. S. P. Bhuvanesh, M. P. Crosnier-Lopez, O. Bohnke, J. Emery and J. L. Fourquet, *Chem. Mater.*, 1999, **11**, 634.
2 N. S. P. Bhuvanesh, M. P. Crosnier-Lopez and J. L. Fourquet, *J. Mater. Chem.*, 1999, **9**, 3093.
3 A. J. Jacobson, J. T. Lewandowski and J. W. Johnson, *J. Less-Common Met.*, 1984, **21**, 92; A. J. Jacobson, J. W. Johnson and

J. T. Lewandowski, *Mater. Res. Bull.*, 1987, **22**, 45; J. Gopalakrishnan and V. Bhat, *Inorg. Chem.*, 1987, **26**, 4299.
4 N. S. P. Bhuvanesh, M. P. Crosnier-Lopez, H. Duroy and J. L. Fourquet, *J. Mater. Chem.*, 2000, **10**, 1685.
5 P. J. Ollivier and T. E. Mallouk, *Chem. Mater.*, 1998, **10**, 2585.
6 M. Richard, L. Brohan and M. Tournoux, *J. Solid State Chem.*, 1994, **112**, 345.
7 J. Rodriguez-Carvajal, Fullprof program: Rietveld Pattern Matching Analysis of Powder Patterns, ILL Grenoble, 1990.
8 D. Babel and A. Tressaud, in *Inorganic Solid Fluorides*, editor: P. Hagenmuller, Academic Press, Inc., New York, London, 1985.
9 K. Toda, S. Kurita and M. Sato, *Solid State Ionics*, 1995, **81**, 267.
10 K. Toda, Y. Kameo, M. Ohta and M. Sato, *J. Alloys Compd.*, 1995, **218**, 228.
11 K. Toda, S. Kurita and M. Sato, *J. Ceram. Soc. Jpn.*, 1996, **104**, 140.
12 K. Toda, Y. Kameo, S. Kurita and M. Sato, *J. Alloys Compd.*, 1996, **234**, 25.
13 K. Toda, T. Honma, Z.-G. Ye and M. Sato, *J. Alloys Compd.*, 1997, **249**, 256.
14 N. E. Brese and M. O'Keeffe, *Acta Crystallogr., Sect. B*, 1991, **47**, 192.
15 J. Laugier and A. Filhol, CELREF program, ILL Grenoble, 1978.
16 R. D. Shannon, *Acta Crystallogr., Sect. A*, 1976, **32**, 751.
17 B. Henssen, S. A. Sunshine, T. Siegrist, A. T. Fiory and J. V. Waszczak, *Chem. Mater.*, 1991, **3**, 528.
18 V. P. Sirotinkin and S. P. Sirotinkin, *Zh. Neorg. Khim.*, 1993, **38**, 1071.